

Wavefunction and level statistics of random two dimensional gauge fields

J. A. Vergés

*Instituto de Ciencia de Materiales de Madrid, Consejo Superior de Investigaciones Científicas,
Cantoblanco, E-28049 Madrid, Spain*

(Received 27 June 1995)

Level and wavefunction statistics have been studied for two dimensional clusters of the square lattice in the presence of random magnetic fluxes. Fluxes traversing lattice plaquettes are distributed uniformly between $-\frac{1}{2}\Phi_0$ and $\frac{1}{2}\Phi_0$ with Φ_0 the flux quantum. All considered statistics start close to the corresponding Wigner-Dyson distribution for small system sizes and monotonically move towards Poisson statistics as the cluster size increases. Scaling is quite rapid for states close to the band edges but really difficult to observe for states well within the band. Localization properties are discussed considering two different scenarios. Experimental measurement of one of the considered statistics –wavefunction statistics seems the most promising one– could discern between both possibilities. A real version of the previous model, i.e., a system that is invariant under time reversal, has been studied concurrently to get coincidences and differences with the Hermitian model.

I. INTRODUCTION

There is a general belief based on Anderson localization theory [1] that all states of two-dimensional (2D) systems are localized in the absence of a magnetic field. The situation is not so clear when time-reversal symmetry is destroyed by a magnetic field. The motion of a single particle in a 2D random magnetic field is attracting strong interest since it is related both to the half-filled Quantum Hall Effect [2,3] and the slave-boson description of high T_c superconductors [4]. The existence of recent experiments measuring transport properties in a static random magnetic field adds considerable interest to this subject [5].

While perturbative renormalization group calculations show that all states are localized [6,7], the eventual presence of an extra term could give rise to a Kosterlitz-Thouless transition from the localized phase to a phase with power law correlations [8]. Numerical simulations have used a variety of forms: the iterative strip method has been used by Sugiyama and Nagaosa [9], Avishai *et al.* [10], Liu *et al.* [11], and Kalmeyer *et al.* [2], analysis of participation ratio has been employed by Pryor and Zee [12] and Kalmeyer and Zhang [2], tails in the density of states have been discussed by Gavazzi *et al.* [13] and Barelli *et al.* [14], a network model has been introduced by Lee and Chalker [15], the diffusion of electrons has been studied by solving the time-dependent Schrödinger equation [16], and finally, Hall conductivity has been used as a way for determining energy regions where extended states dominated in the thermodynamic limit [17]. Loosely speaking, states *look* extended in finite samples as soon as the edge of the band is left and a definite answer is quite difficult. Therefore, the most extended conclusion is that a mobility edge separates localized states from extended or critical states. On the contrary, Sugiyama and Nagaosa [9] conclude that *all* states are localized in random magnetic fields based on

the non-existence of a second branch in the scaling function whereas the same conclusion is reached by Lee and Chalker [15] based on finite values of the localization length obtained in the semiclassical limit described by their model.

In this work, I present numerical evidence showing that, in the presence of random fluxes, states scale towards random (Poisson) statistics everywhere in the band. Several standard statistics (wavefunctions amplitude statistics, nearest neighbor spacing statistics and number variance) are used in conjunction with other criteria (for example, spatial extension of wavefunctions as given by the participation ratio) to show a systematic tendency towards Poisson statistics (the one that characterizes systems with a spectrum formed by exponentially localized states) as the size of the random samples increases. Scaling is quite rapid near the band edge where states "look" exponentially localized whereas it seems to follow a logarithmic law near the band center where states "look" fractal [18]. Nevertheless, since my analysis is based on statistical magnitudes, the eventual existence of a countable set of extended states can not be disproved. In other words, the results presented in the next Sections prove that states scale towards localization *on average*.

Recent results regarding level statistics can be found in the literature [14,19]. Most of them deal with the characterization of a new universal distribution function that would be appropriate at the metal-insulator transition. As the results presented in the rest of the paper show, signs suggesting the existence of a critical energy (mobility edge) at which scaling changes sign have not been found. *Scaling flows in the same direction in all energy regions*. The paper is organized as follows. Section II defines the model that has been numerically solved in the paper, Section III gives the main results grouped under three subjects (Density of states, wavefunctions and level statistics) and finally, main conclusions are collected in

the last Section.

II. LATTICE MODEL

The Hamiltonian describing random gauge fields on a $L \times L$ cluster of the square lattice is :

$$\hat{H} = -t \sum_{\langle ll' \rangle} e^{2\pi i \phi_{ll'}} \hat{c}_l^\dagger \hat{c}_{l'} \quad , \quad (1)$$

where \hat{c}_l^\dagger creates an electron on site l , l and l' are nearest-neighbor sites, and $-t$ is the hopping energy (hereafter $t = 1$ is chosen). The flux through a given loop S on the lattice is $\Phi_S = \sum_{\langle l, l' \rangle \in S} \phi_{ll'}$ measured in units of flux quantum $\Phi_0 = \frac{hc}{e}$. Link fields satisfy $\phi_{ll'} = -\phi_{l'l}$. Although some checks have been performed for the Meissner phase [13] (link fields uniformly, randomly distributed in the interval $[-\frac{1}{2}, \frac{1}{2}]$), the bulk of the calculations have been done for the Debye phase in which uncorrelated fluxes are randomly selected from the interval $[-\frac{1}{2}, \frac{1}{2}]$. Notice that in any case, the situation of maximum possible disorder is considered except when the density of states is analysed as a function of disorder. Model (1) will be called RMF (Random Magnetic Fluxes or Random Magnetic Field) model in the rest of the paper.

In order to recover standard results, I have always run checks for a *real* version of Hamiltonian (1). To this end, link field values are restricted to 0 and $1/2$ and chosen randomly. The model describes a square lattice in which the hopping integral is constant in absolute value but takes random signs. This model will be shortly mentioned as RHS (Random Hopping Signs) model. Standard localization theory should apply to this model. Both models are equivalent for a particular choice of random fluxes; when $\phi_{ll'}$ is always equal to $\frac{1}{4}$ but has random sign, hopping integrals take random $\pm i$ complex values. Thanks to the bipartite character of the square lattice, this Hamiltonian can be made real: it suffices a canonical transformation of all operators on one of the sublattices from \hat{c}_l to $i\hat{c}_l$. In this way, this particular complex Hamiltonian is described by the same matrices as the RHS model. This case provides an overlap between real random Hamiltonians that according to standard theory show complete localization and a Hamiltonian with complex eigenfunctions.

III. RESULTS

A. Density of states

One of the easiest ways allowable to characterize the effect of disorder is the density of states (DOS):

$$N(E) = \frac{1}{N} \sum_{\alpha} \delta(E - E_{\alpha}) \quad (2)$$

where the sum runs over all eigenstates of the system. For arbitrary disorder $\{\phi_{ll'}\}$ the eigenvalues of Hamiltonian (1) lie in the interval $[-4, 4]$. Moreover, there is also an exact symmetry on a bipartite lattice like the square lattice. For every eigenfunction of energy E there is an eigenfunction of energy $-E$ whose amplitudes have opposite sign on one of the sublattices. As a consequence, the density of states is symmetric about $E = 0$. The same symmetry forces the existence of an eigenstate of zero energy in clusters of an odd number of sites.

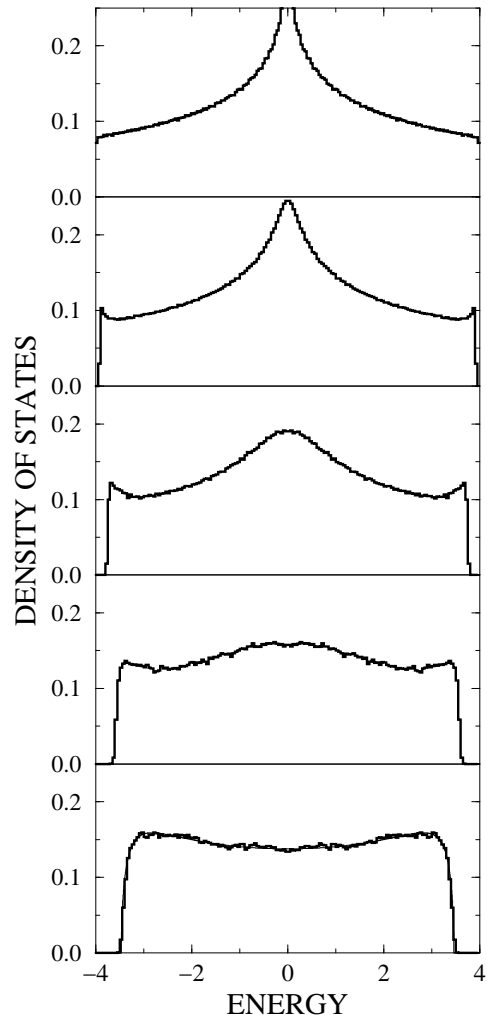


FIG. 1. Evolution of the density of states as the interval $[-\phi_{\max}, \phi_{\max}]$ from which random values of the flux are selected increases. From top to bottom: ideal system, $\phi_{\max} = \frac{1}{8}, \frac{1}{4}, \frac{3}{8}$ and $\frac{1}{2}$. The DOS of a Bethe lattice of coordination equal to four has been plotted (continuous line) in the bottom panel to allow comparison with the RMF result.

Generally, an average over disorder realizations is done in order to get a smooth result. Averaging is particularly important when Anderson model is studied for large disorder because band width increases and the number of states per energy unit diminish. Since the disorder given

by Hamiltonian (1) systematically decreases the width of the band, the study of only one large sample suffices to get nice results. Fig.(1) shows the evolution of the density of states obtained for a 200×200 system as disorder (random fluxes distributed in the interval $[-\phi_{\max}, \phi_{\max}]$) increases. A small amount of disorder destroys the logarithmic singularity at the center of the regular system and shrinks somewhat the band. Peaks appear near the band edges due to some kind of accumulation of states due to the band shrinkage. Finally, a smooth curve is obtained for the maximum possible amount of disorder: random fluxes between $-\frac{1}{2}$ and $\frac{1}{2}$. In this case, the density of states of a Bethe lattice of coordination equal to four:

$$N(E) = \frac{2}{\pi} \frac{\sqrt{12 - E^2}}{16 - E^2} \quad (3)$$

gives a very good approximation to the random result (it is difficult to distinguish between histogram and continuous curve in the bottom panel of Fig.(1)). Although the characterization and deep understanding of the peak appearing close to the edges at small disorder deserves further study, the rest of the paper is devoted exclusively to the case of maximum disorder (bottom panel of Fig.(1)).

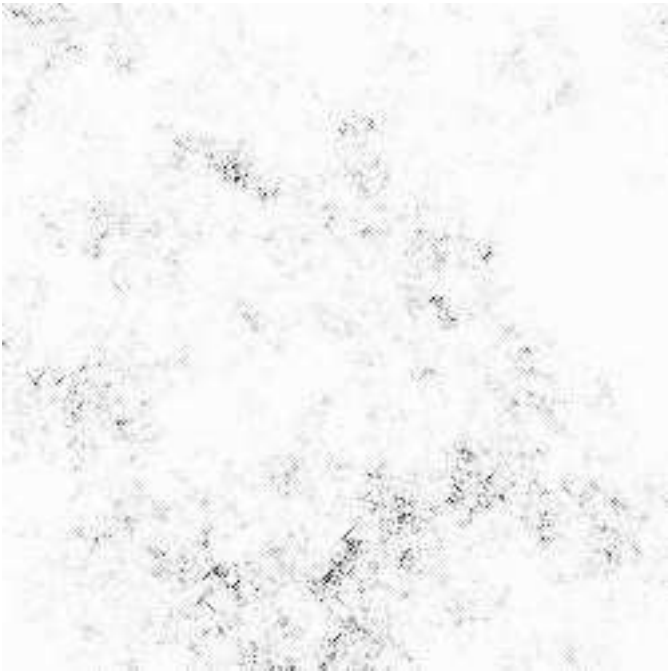


FIG. 2. Typical "extended" wavefunction of a 250×250 cluster and energy $E \approx -\pi/50$.

B. Wavefunctions

Wavefunctions can be obtained using standard algorithms for Hermitian band matrices [20] if the size of the

matrix is not too large (a typical workstation can deal with a 200×200 cluster, i.e., with a 40000×40000 matrix if only eigenvalues are calculated but only with a 64×64 system (a matrix of dimension equal to 4096) if eigenvectors should be obtained). On the other hand, inverse iteration [21] allows the calculation of particular eigenvectors. The algorithm starts with some random values for the components of the wavefunction ψ_0 of energy E and proceeds as follows:

$$\begin{aligned} \psi_1 &= (E - \hat{H})^{-1} \psi_0 \\ \psi_2 &= (E - \hat{H})^{-1} \psi_1 \\ &\dots \end{aligned} \quad (4)$$

Convergence is reached when $|\psi_i - \psi_{i-1}|$ is smaller than some tolerance ϵ ($\epsilon = 10^{-8}$ works fine in double precision). Energy should be updated after some number of cycles (about 10):

$$E_i = \langle \psi_i | \hat{H} | \psi_i \rangle \quad .$$



FIG. 3. Typical "localized" wavefunction of a 250×250 cluster and energy $E \approx -\pi/50$.

Taking advantage of the band structure of the Hamiltonian, eigenstates for clusters as large as 300×300 can be obtained using standard linear algebra subroutines. Sometimes larger systems are accessible: for example, since $E = 0$ is always an eigenenergy of Hamiltonian (1) when the number of sites is odd, total number of iterations is greatly reduced and eigenvectors for 399×399 clusters can be obtained. The computational thresholds

that have been given refer to complex Hermitian matrices. Somewhat larger systems can be studied for the real version of model (1).

Wavefunctions produced by Hamiltonian (1) present a great richness. We get *bona fide* exponentially localized wavefunctions for energies close to the band edges, almost localized wavefunctions (i.e., wavefunctions that show non vanishing amplitudes in a small part of the cluster) in any part of the energy spectrum, quasi one-dimensional eigenstates in many cases and also, quasi extended wavefunctions in the main part of the spectrum. Figs.(2) and(3) show typical results at cluster sizes at which only inverse iteration allows the calculation of specific eigenstates [21]. Wavefunctions are represented through a 256 values grey scale in which darker means larger values of $|\psi_l|^2$ being ψ_l the wavefunction amplitude on site l . Although a large collection of such wavefunctions have been compiled, it is clear that the simple display of them does not help to the analysis of localization. Therefore, I have use standard tools to analyse their extension and the way they behave as the size of the sytem is increased.

1. Participation ratio

A good measure of the spatial extension of an eigenstate is given by the participation ratio:

$$P = \left(\sum_{l=1}^{L \times L} |\psi_l|^4 \right)^{-1}, \quad (5)$$

where ψ_l is the amplitude of wavefunction on site l . P can be understood as the number of sites covered by the wavefunction and reaches a maximum finite value for localized states. In order to avoid systematic errors due to the use of a biased definition, I have also tried alternative definitions of the spatial extension covered by a wavefunction. One is given in Casati and Molinari work [22]:

$$C = \exp \left(- \sum_{l=1}^{L \times L} |\psi_l|^2 \log(|\psi_l|^2) \right), \quad (6)$$

a definition of the number of sites asociated to a wavefunction that emphasizes small amplitudes and gives consequently larger values than the previous definition. Still another definition is based in the basic understanding of $|\psi_l|^2$ as the probability of finding the particle at site l . We proceed in two steps: (i) weights $|\psi_l|^2$ are ordered in decreasing magnitude and (ii), S is defined as the number of ordered weights that have to be added to reach some percentage of the total weight 1 of the state. I have tried different percentages to learn that this simplest definition gives results for S that are practically identical to C when 99% of the total weight is considered. Using 90%

as the cutoff, results closely follow those obtained using the standard P definition. This knowledge gave me further confidence in the reliability of the usual definitions of number of sites covered by a wavefunction.

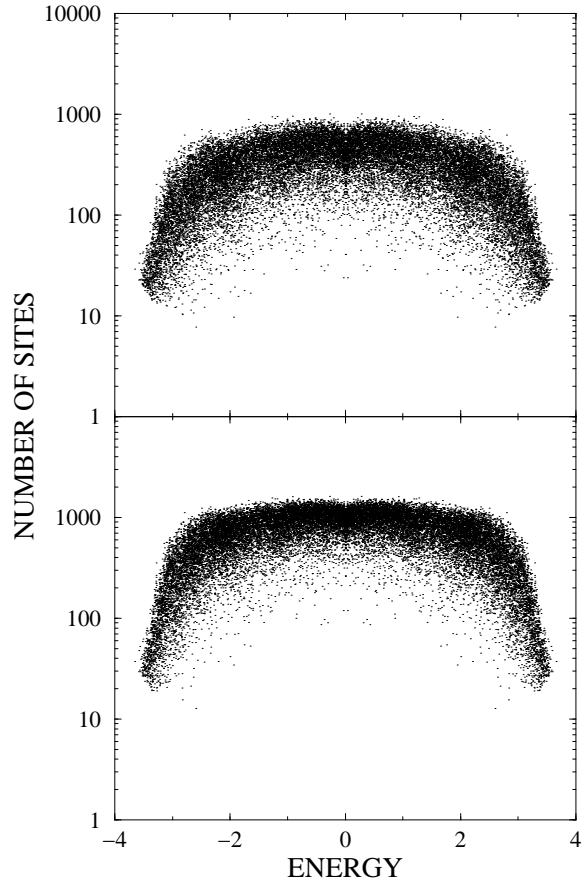


FIG. 4. Number of sites for all states of seven samples of 64×64 size. Top: *standard* definition of the participation ratio(5). Bottom: Logarithmic definition(6).

Fig.(4) and Fig.(5) show both P and C for a collection of the largest clusters for which the complete set of eigenenergies and eigenvectors can be obtained using my limited computing facilities. Schwarz algorithm for symmetric or Hermitian band matrices has been used [20]. These results show that spatial extension is small near band edges but increases quickly towards the band center. In fact, the behavior is really sharp for the complex RMF model. One can be tempted to speak about some kind of pseudo-mobility edge at these energies ($\sim \pm 3$) where spatial extent sharply increases. In fact these energies coincide with the values given in the literature as the limits of a reliable calculation of the localization length (see, for example, the paper by Sugiyama and Nagaosa [9]). Moreover, while states well within the band show a steady power law increase in their spatial extension, states close to the edges *do not* extend as the size of the system is increased.

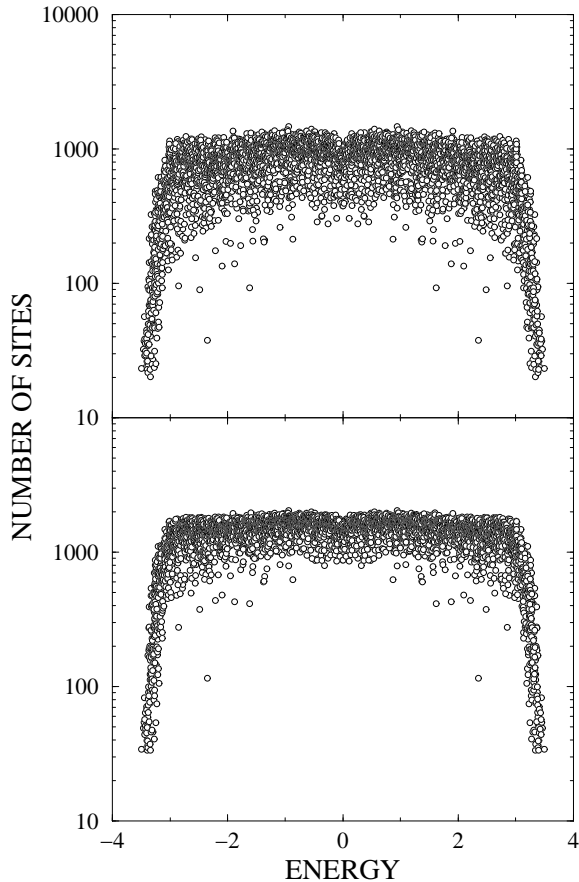


FIG. 5. Number of sites for all states of two samples of 58×58 size. Top: *standard* definition of the participation ratio(5). Bottom: Logarithmic definition(6).

The scaling behavior of the spatial extension of states has been carefully analysed at particular energies. In this analysis inverse iteration is used and therefore, eigenstates for much larger systems are available. Fig.(6) collects results for RHS model at several energies while Fig.(7) shows spatial extension results for RMF model just at the band center. Let me begin the discussion with some comments about the results displayed in Fig.(6). Several energies covering different parts of the spectrum have been chosen. While it is clear that the growth of the spatial extension is bound in the lower part of the band ($E = -3.4$ and perhaps $E = -3$), results at energies well within the band show eigenstates that extend more and more as the system size increases. Of course, the validity of this conclusion is limited by the sizes that are reachable by a numerical study (the largest cluster analysed in this case is 210×210). Nevertheless, a quadratic fit to the log-log plot shows a small negative curvature that indicates that after a region in which $\langle P \rangle \sim L^\alpha$ ($\alpha \leq 2$), a region of true exponential localization of wavefunctions could follow. Again a word of caution is in order at this point: the inference of the asymptotic behavior of coverage from the analysis of a limited range of sizes is really

a hard question in any numerical study. Therefore, the only conclusion that seems to be sure is that coverage increases following a power law with an exponent smaller than 2 *at the most*.

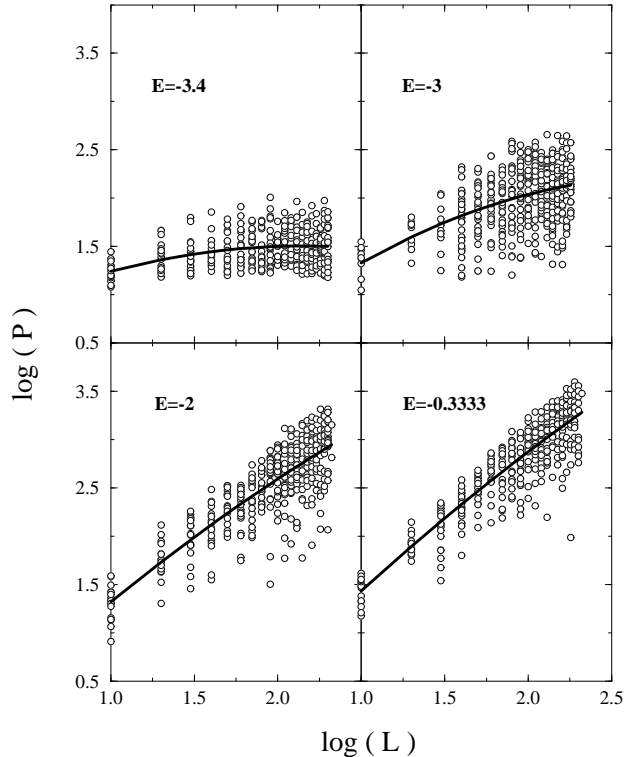


FIG. 6. Spatial extension of eigenstates produced by the real version of Hamiltonian (1) at different energies. Circles give the value of $\log(P)$ of the state that is closest to the selected energy for each sample of a set of realizations of disorder. L is the cluster size. Solid lines are quadratic fits to the log-log values.

A similar analysis is displayed in Fig.(7) for the Hermitian Hamiltonian. Participation ratios for states at the band center are given for increasing cluster sizes. In that case, the maximum size allowed by our computing capabilities is 399×399 . Even for this system size, the number of sites covered by eigenstates at the band center is following on average a law close to $\langle P \rangle \sim L^{1.6}$. The curvature of a quadratic fit to the log-log data shows again negative –although really small– curvature (solid line of Fig.(7)). So, we are forced to conclude that numerical methods based in the study of the scaling properties of individual states are not enough to show exponential localization in 2D random gauge fields.

2. Fractal dimension

Fractal dimension has been defined as:

$$\alpha = \frac{d \log(P)}{d \log(L)} \quad . \quad (7)$$

It characterizes energies or system sizes for which the number of sites covered by eigenstates increases following a power law (Number of sites $\propto L^\alpha$). It has been calculated for the whole spectrum using energy averaged values for the number of sites and two different system sizes to calculate the derivative. In other words, we have:

$$\alpha = \frac{\Delta \log \langle P \rangle}{\Delta \log \langle L \rangle} . \quad (8)$$

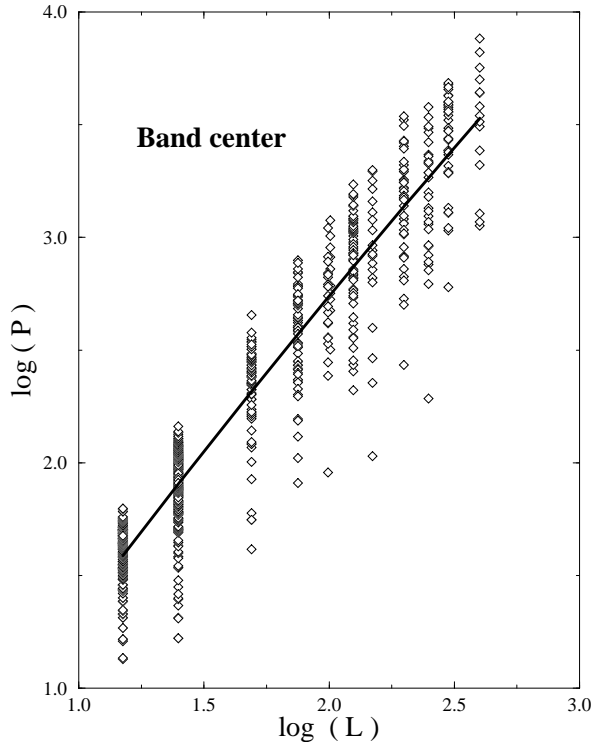


FIG. 7. Spatial extension of eigenstates produced by Hamiltonian Eq.(1) at the band center. Diamonds correspond to different realizations of disorder for several sizes ($L \times L$ cluster). Solid line is a quadratic fit to the log-log values.

Fig.(8) gives our numerical results for both models. Sizes $L = 32, 64$ have been used for RHS model whereas sizes $L = 24, 48$ did the work for the more difficult RMF model. It can be seen that although the overall behavior is similar for both models, the increase to ≈ 1.8 is so sharp for the RMF model that the idea of some critical energy separating exponentially localized states from states following a power law decay could be considered.

The fact that fractal dimension for averages of the coverage P is below 1.8, together with the more detailed results at particular energies shown in the previous subsection, proves overall localization *at least in a power law way*:

$$\frac{\langle P \rangle}{L^2} \rightarrow 0 .$$

This behavior is in striking contrast with the result that applies to wavefunctions of the GUE:

$$\frac{\langle P \rangle}{N} \rightarrow \frac{1}{3} ,$$

where the total number of sites N plays the role of L^2 in the previous expression. For the same reason, localization is also present in the simplified RHS model for which fractal dimension is always less than 1.4. Actually, states are less extended for this model.

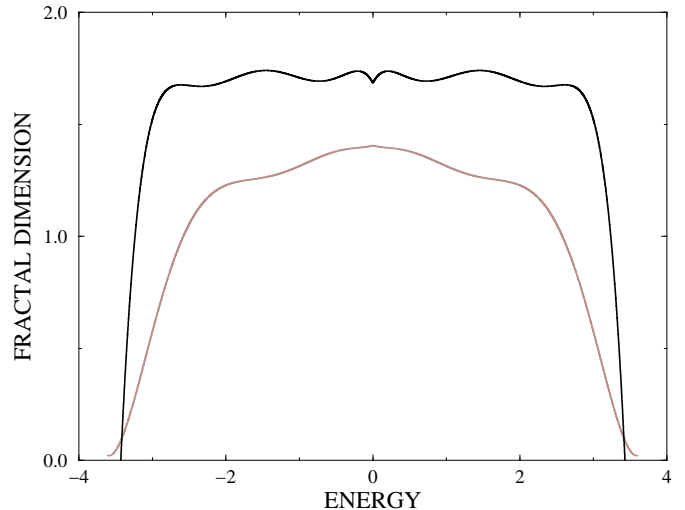


FIG. 8. Fractal dimension of both models (RHS: grey line; RMF: black line) as a function of the position of states within the band.

3. Wavefunction amplitude statistics

Wavefunction statistics measures the spatial variation of eigenfunctions over the system under study. Crystalline wavefunction have constant amplitude $1/N$ whereas wavefunction of disordered or chaotic systems show large fluctuations. The wavefunction statistics of the canonical Gaussian ensembles is given by the corresponding Porter-Thomas distribution [23]. In particular, we have

$$f(t) = \frac{1}{\sqrt{2\pi t}} \exp(-t/2) , \quad (9)$$

for the Gaussian Orthogonal Ensemble, where t is the squared wavefunction amplitude divided by its mean value, i.e., ($t = N\psi(\mathbf{r})^2$) being N the number of sites. Graphical representation is improved if variable $x = \log(t)$ is used instead of t . We get:

$$g(x) = \frac{1}{\sqrt{2\pi}} \exp \left\{ \frac{1}{2} [x - \exp(x)] \right\} . \quad (10)$$

On the other hand, we have:

$$f(t) = \exp(-t) \quad , \quad (11)$$

for the Gaussian Unitary Ensemble, where t is the squared wavefunction amplitude divided by its mean value, i.e., ($t = N\psi(\mathbf{r})^*\psi(\mathbf{r})$). Doing the same variable transformation as before, we get:

$$g(x) = \exp(x - \exp(x)) \quad . \quad (12)$$

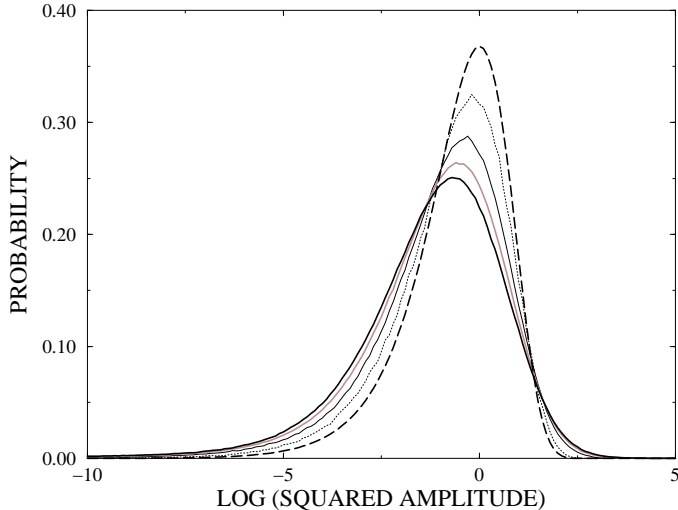


FIG. 9. Wavefunction statistics of RMF model. Distribution of wavefunction weight for i) an average over all states of 256×8 samples (dotted line), ii) an average over all states of 64×16 samples (solid line), iii) an average over all states of sixteen 32×32 samples (grey thick solid line) and, iv) an average over all states of two 58×58 samples (black thick solid line). GUE Porter-Thomas distribution is given for comparison (dashed line).

Deviations from these canonical distributions have been recently calculated by Falko and Efetov [24]. Their work applies to pre-localized states in disordered conductors. Numerically, it is a simple task getting deviations from universal behavior. Fig.(9) shows the rapid deviation of RMF wavefunction statistics from the corresponding Porter-Thomas distribution (Eq.(12)) as soon as eigenfunctions of medium-size matrices are considered. In this calculation, all states –regardless their energy– have been used to compute the probability density. Close to the maximum capability of my computer (58×58 clusters), it can be seen that the ratio of evolution of wavefunction statistics with size is decreasing.

The divergence of wavefunction statistics from the corresponding Porter-Thomas distributions shown in the last Figure is confirmed by the calculation of wavefunctions of much larger clusters close to a fixed energy (I have used inverse iteration starting at $E = -\pi/50$ trying to get unbiased eigenstates that could exist at special energies). Fig.(10) shows selected results for RHS

model while Fig.(11) gives RMF results. In both cases, the same clear tendency of diverging from Porter-Thomas statistics as size increases, can be seen. Nevertheless, the distance to a *typical* statistics produced by exponentially localized wavefunctions is still large (thick solid line of Fig.(11) shows wavefunction statistics at the band edge). Notice that exponential localization implies a statistics that shifts towards left (smaller weights are more probable) as the size of the system increases beyond the localization length.

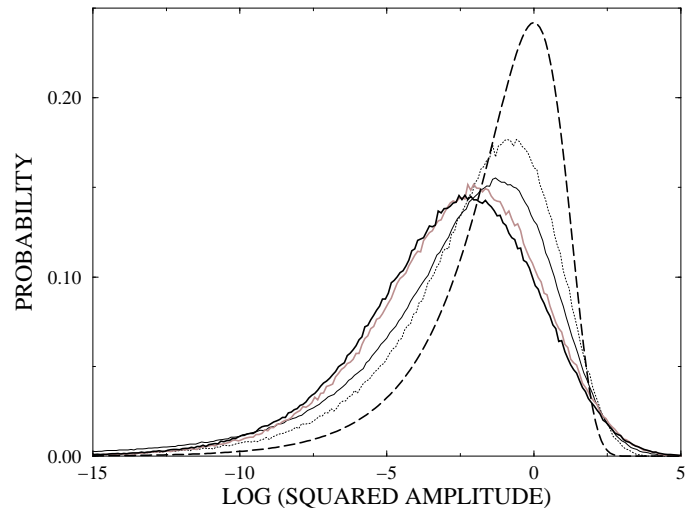


FIG. 10. Wavefunction statistics of RHS model. Distribution of wavefunction weight for i) an average over all states of sixteen 16×16 samples (dotted line), ii) an average over all states of four 32×32 samples (solid line), iii) an average over fifteen states of energy $E \approx -\pi/50$ obtained for different 200×200 clusters (grey thick solid line) and, iv) an average over ten states of energy $E \approx -\pi/50$ obtained for different 300×300 clusters (black thick solid line). GOE Porter-Thomas distribution is given for comparison (dashed line).

C. Level statistics

1. Nearest neighbor spacing statistics

Level statistics has been recently used to characterize the properties of spectra near the mobility edge [19]. It is well known that the distribution of nearest neighbor spacings is of the Wigner-Dyson type [25] when particles move through the whole slightly disordered sample and changes to Poisson when states become exponentially localized. Simplifying the argument, we can say that only states localized in different spatial regions do not interact through the Hamiltonian and are, therefore, allowed to lie at the same energy. According to this theory, level statistics should move towards Poisson as the size of the system increases *whenever* states are localized in the thermodynamic limit whereas it should move

towards the corresponding Wigner-Dyson distribution if states are extended in the infinite system [26].

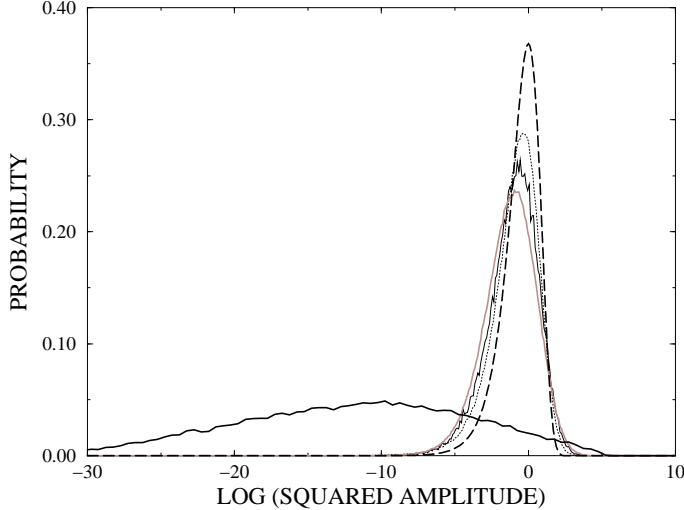


FIG. 11. Wavefunction statistics of RMF model. Distribution of wavefunction weight for i) an average over all states of sixteen 16×16 samples (dotted line), ii) an average over forty states of energy $E \approx -\pi/50$ obtained for different 50×50 clusters (solid line), iii) an average over six states of energy $E \approx -\pi/50$ obtained for different 300×300 clusters (grey thick solid line) and, iv) an average over twenty states of energy $E \approx -3.4$ obtained for different 50×50 clusters (black thick solid line). GUE Porter-Thomas distribution is given for comparison (dashed line).

Fig.(12) shows the results of a standard analysis of nearest neighbor spacings produced by the RMF model. The statistics of small clusters (144 sites) closely follows Wigner surmise whereas statistics of the largest system that we can analyse (40000 sites) shows a small but clear deviation from GUE statistics. On the other hand, larger scaling features can be observed if the level spacing distribution obtained at the lower part of the spectrum of the RHS model is analysed (see Fig.(13)). Level statistics for small sizes (empty circles) reasonably follows Wigner-Dyson distribution (dashed line) whereas larger sizes give rise to a distribution (filled circles) that is approaching Poisson distribution (dotted line).

2. Scaling of the variance of the spacing distribution

Since the visual inspection of nearest neighbor spacing distribution is not a quantitative way of analysing their evolution with system size, I have selected the variance of the distribution as the scaling magnitude. Matrices belonging to the GOE (GUE) give a distribution of variance equal to 0.286 (0.180) [27], whereas the variance of the Poisson distribution is 1. So, a continuous increase of the width of the level spacing distribution (measured here by its variance) should denote the path extended-

to-localized followed by wavefunctions. Large samples of nearest neighbor spacings has been obtained by direct diagonalization of Hamiltonian matrices obtained for random realizations of disorder. The total number of levels has been maintained almost constant (~ 200000 for RHS model and ~ 480000 for RMF model) as the size of the square cluster has been increased from 12×12 to 200×200 .

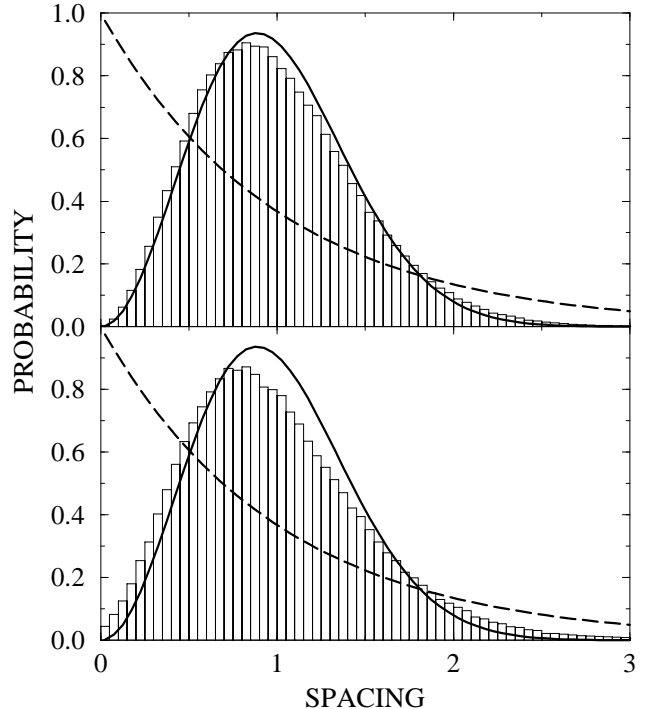


FIG. 12. Top panel: Distribution of nearest neighbor spacings obtained for 4096 randomly generated 12×12 clusters (histogram). Bottom panel: Distribution of nearest neighbor spacings obtained for eleven randomly generated 200×200 clusters (histogram). Poisson (dashed line) and Wigner-Dyson (solid line) distributions are shown for comparison purposes.

Firstly, I present the results obtained for the variance of the whole sets of spacings. They are given in Fig.(14) for both models together with the results obtained for rectangular clusters (these are the only results for this cluster shape presented in the paper). While scaling is obviously towards localization for $2 \times L$ systems, asymptotic values for squares (RHS model) and circles (RMF model) cannot be inferred in a unique way. A good fit is obtained using the following model curve:

$$\sigma = A + C_1/L + C_2/\log(L) + C_3/(L \log(L)) + C_4/L^2 + C_5/\log(L)^2, \quad (13)$$

where σ means variance and L is the cluster size. Unfortunately, while results for RHS point towards a value $A = 1$ in a three parameter fit (ideal localization of all eigenstates), RMF results for A are not so well defined (the number of parameters makes appreciable dif-

ferences) but point to an A value smaller than 1 although a five parameter fit with fixed $A = 1$ also goes through all circles. If this overall fit could be taken quite seriously, it would mean that some percentage of the total number of states (about fifty percent since $A \approx 0.6$) does not follow a random statistics even in the thermodynamic limit. I will come back to the discussion of this point after the presentation of all results.

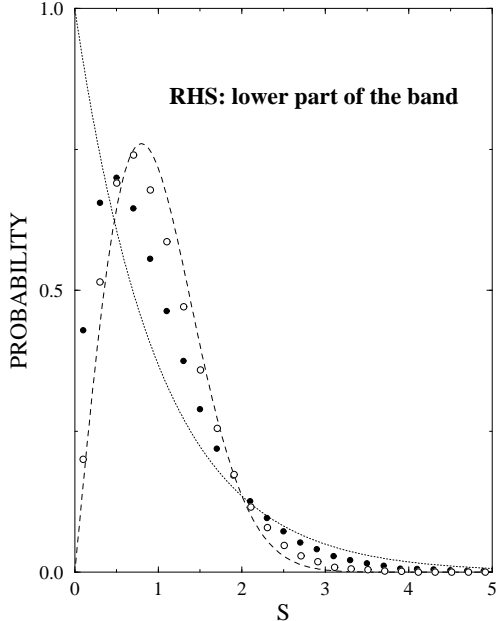


FIG. 13. Distribution of nearest neighbor spacings in the lower part of the band produced by the real version of Hamiltonian (1) for two different system sizes: open circles correspond to an ensemble of 12×12 clusters whereas filled circles show the distribution for an ensemble of 200×200 clusters. Poisson and Wigner GOE distributions are shown for comparison.

Secondly, an analysis that takes into account the energy region from which level spacings originate has been done. Level spacings have been grouped in seven sets corresponding to seven energy regions and the variance of the corresponding distributions has been calculated. Fig.(15) shows the flow towards Poisson statistics followed by the level statistics within the different energy regions. Scaling in the lower part of the band shows a rapid tendency to localization while states near the band center show a much slower ratio. This behavior easily explains why localization is easily detected near the band edges but is almost invisible near the band center (see Fig.(6)).

Numerical analysis is still more difficult for the Hermitian RMF model since scaling towards localization is much slower for this model. Remember that the number of level spacings is large and almost constant (~ 480000) for all considered system sizes. In this case, the variance should start close to the value of 0.180 that corresponds to the nearest neighbor level spacing distribution given by

matrices of the Gaussian Unitary Ensemble [27]. Fig.(16) shows the evolution of the variance of nearest neighbor level spacings within different energy regions. As before, states close to the band edge localize at small sizes (≤ 200) but the body of wavefunctions shows a much slower scaling behavior (compare the scales of y-axis in Figs. (15) and (16)). Since the increase of the variance in a given energy range is roughly the same for the four increases of the cluster size, a logarithmic dependence of the variance with the system size could be inferred (Notice that the number of sites is increased by a factor of four in each step). If this were the case, that would imply that only huge clusters would show exponential localization of wavefunctions, and consequently, Poisson statistics of level spacings.

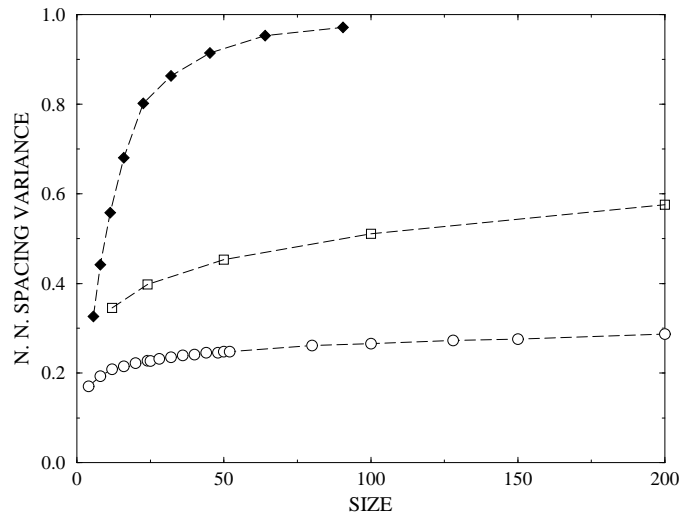


FIG. 14. Scaling behavior of nearest neighbor spacing variance as a function of cluster size. Squares give the evolution of the variance calculated for the whole band of square clusters of side L for the RHS model, circles represent the same magnitude for the RMF model and, filled diamonds give the scaling behavior for a $2 \times L$ cluster of RMF model (in this case the size is not the length of the square side as before but $\sqrt{2L}$)

In conclusion, although the scaling law at the studied sizes seems to be logarithmic for the main part of the band, numerical results show without doubt that the whole spectrum is scaling towards larger values of the variance, and therefore, towards localization. In any case, level statistics of both RHS and RMF models *is not scaling* towards the corresponding Wigner-Dyson statistics. The only alternative to a complete scaling towards a random distribution of levels, i.e., towards exponential localization of the whole spectrum, is the existence of some new non-universal statistics for this Hamiltonian models. This possibility will be further discussed in the last Section.

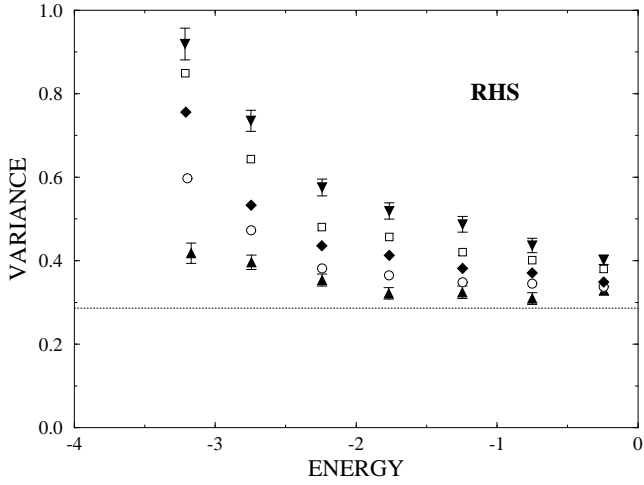


FIG. 15. Variance of the nearest neighbor spacing distribution of the RHS model as a function of the energy plotted for increasing sizes of the cluster: the side of the square cluster equals 12, 24, 50, 100, and 200 for up triangles, circles, diamonds, squares, and down triangles, respectively. The upper half of the band shows identical behavior. Error bars are given for the smallest and the largest cluster sizes.

3. Number variance statistics

Number variance statistics measures fluctuations in the number of levels that appear in an interval of fixed length. In this case, the statistical variable is n (number of states in an interval of renormalized length equal to s) and its variance $\langle (n - \langle n \rangle)^2 \rangle$ is calculated. Wigner-Dyson ensembles produce spectra of remarkable rigidity which in turn means small values of the number variance [27]. On the other hand, a random sequence of levels gives rise to a number variance equal to the length of the interval. The advantage of using this statistics to characterize a level sequence is that long range correlations are explicitly shown. Number variance statistic is also closely related with the variance of the distance of one level to its n -th neighbor [28].

In accordance with the analysis done in previous subsections, number variance shows an increasing separation of RHS (RMF) statistics from Wigner-Dyson GOE (GUE) values as the size of the system increases. Since it is really not plausible that this tendency could change beyond some critical size, we can conclude that the overall spectra flows towards Poisson statistics, i.e., towards localization for both RHS and RMF models. Although not shown in the paper, when the band is analysed grouping levels within different energy regions, the result of previous subsection is recovered: scaling towards random statistics of states close to the band edges is quite rapid whereas scaling is much slower near band center. Once again, the quasi mobility edge defined by results given in Figs.(4), (5) and (8) signalizes the change of behavior.

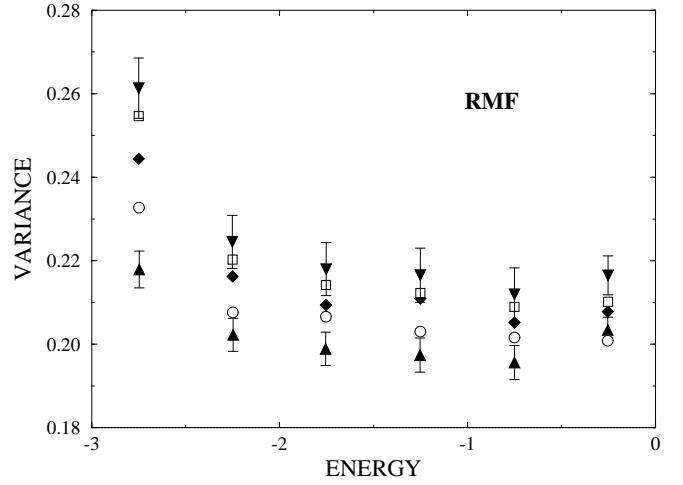


FIG. 16. Variance of the nearest neighbor spacing distribution of the RMF model as a function of the energy plotted for increasing sizes of the cluster: the side of the square cluster equals 12, 25, 50, 100, and 200 for up triangles, circles, diamonds, squares, and down triangles, respectively. Error bars are given for the smallest and the largest cluster sizes.

IV. DISCUSSION

The discussion of the results presented in Section III can be done according to two different scenarios. Within the first one, the existence of only two fixed points for the flow of eigenstates of a matrix belonging to one of the universality classes is assumed. In our case, since matrices describing RMF model (Eq.(1)) are Hermitian (the system is not invariant under time reversal), the two fixed points are: (i) the one described by the Gaussian Unitary Ensemble (i.e., Wigner-Dyson statistics of levels sequence, Porter-Thomas statistics for wavefunctions, etc.) and (ii), the one corresponding to localization (Poisson statistics for the random sequence of levels, increment of the number of sites having a vanishing wavefunction weight, etc.). If this assumption is true, all numerical results prove overall scaling towards localization. Moreover, the same trend has been proved for states belonging to different energy regions. Nevertheless, in spite of the clear and extense numerical evidence supporting this conclusion, one word of caution is necessary. Since my analysis is exclusively based on the scaling of averaged magnitudes, there is always the possibility that a countable number of states of vanishing weight in averages do not follow overall scaling and remain extended. This conclusion is in agreement with the widely accepted point of view that states are localized in infinite two-dimensional systems no matter how small the degree of disorder is [1].

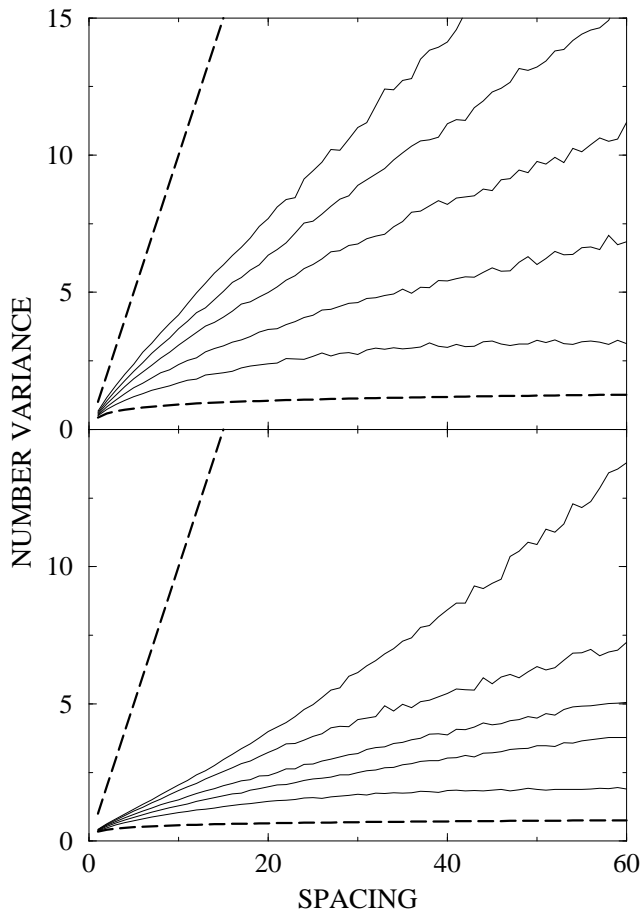


FIG. 17. Number variance as a function of spacing for both RHS model (upper panel) and RMF (lower panel). Results for 12×12 , 24×24 , 50×50 , 100×100 and, 200×200 square clusters are given as continuous lines that monotonically go from the corresponding Gaussian ensemble result (lower dashed line) towards the straight dashed line that gives the Poissonian statistics corresponding to a random level sequence.

On the other hand, a second scenario is also possible. States close to the band edges are certainly exponentially localized but it could happen that states within the band were extended, at least in a loose form: states whose spatial extension increases as $P \sim L^\alpha$, with $\alpha < 2$, cover an infinite number of sites for $L \rightarrow \infty$ although the percentage of visited sites relative to the total number of sites vanishes: $P/L^2 \rightarrow 0$. In this case, the observed flow towards random (localized) statistics of all measured statistical magnitudes could eventually stop at certain "new" fixed point. Under this assumption, statistics would start at Wigner-Dyson fixed point because small matrices are *almost* filled and separate from this point for larger matrices. All numerically observed effects would be assigned to finite size effects.

One can give further plausibility to the second option using results obtained for an ensemble of random *real* band matrices. It has been shown both numerically [22] and mapping the problem into a non-linear supersym-

metric σ model [29] that the average number of sites visited by a wavefunction is $\sim b^2$ being b the band width. This gives a typical localization length of the order of b . In our case, we are indeed dealing with band matrices of a particular kind: Hamiltonian (1) on a $L \times L$ cluster of the square lattice gives band matrices of width L with only four nonzero matrix elements within the band. As a consequence, a localization length $\xi \sim L$ could be expected for RHS model and also, presumably, for RMF model. If this were the case, I think that such a large localization length (of the order of the sample size) can only be understood as signalling some kind of "geometrical" or fractal localization as the one described in the previous paragraph.

Incidentally, this second scenario would be more interesting from the point of view of experimental mesoscopic physics than the canonical one. Instead of measuring *universal* statistics like Wigner surmise corresponding to the GUE, a *new* although non-universal statistics could be obtained (Compare, for example, Wigner surmise in the bottom panel of Fig.(12) with the distribution corresponding to 40000 sites described by the RMF model).

In summary, there are unfortunately two different but internally consistent explanations of the whole set of numerical results. Either the number of fixed points is limited to the well known universality classes of non-interacting systems and then random magnetic fluxes imply localization at all energies or a new fixed point exists for the particular type of random band matrices ensemble considered in this paper and then the major part of eigenstates would exhibit fractal behavior instead of standard exponential localization.

ACKNOWLEDGMENTS

I gratefully acknowledge the hospitality of the Condensed Matter Theory Group of M.I.T. where this work was begun and people of the Applied Physics Department of the University of Alicante where the work was almost finished. I thank E. Mucciolo for giving me the program that obtains the level spacing distribution from a set of eigenenergies and M. Ortuño for insisting about the necessity of using alternative ways to characterize localization. This work has been partially supported by Spanish CICYT (grant MAT94-0058-C02).

-
- [1] E. Abrahams, P. W. Anderson, D. C. Licciardello, and V. Ramakrishnan, Phys. Rev. Lett. **42**, 673 (1979).
 - [2] V. Kalmeyer and S. C. Zhang, Phys. Rev. B **46**, 9889

- (1992); V. Kalmeyer, D. Wei, D. P. Arovas, and S. C. Zhang, Phys. Rev B **48**, 11095 (1993).
- [3] B. I. Halperin, P. A. Lee, and N. Read, Phys. Rev B **47**, 7312 (1993).
- [4] L. B. Ioffe and A. I. Larkin, Phys. Rev B **39**, 8988 (1989), P. A. Lee, Phys. Rev. Lett. **63**, 680 (1989), N. Nagaosa and P. A. Lee, Phys. Rev. Lett. **64**, 2450 (1990), and M. Grilli and G. Kotliar, Phys. Rev. Lett. **64**, 1170 (1990),
- [5] A. K. Geim, S. J. Bending, and I. V. Grigorieva, Phys. Rev. Lett. **69**, 2252 (1992), A. Smith, R. Taboryski, L. Thiel-Hansen, C. Sorensen, P. Hedegaard, and P. Lindelof (unpublished) and F. Mancoff, R. Clarke, C. Marcus, S. C. Zhang, K. Campman, and A. Gossard (unpublished).
- [6] S. Hikami, Prog. Theor. Phys. Suppl. **107**, 213 (1992).
- [7] A. G. Aronov, A. D. Mirlin, and P. Wölfle, Phys. Rev B **49**, 16609 (1994).
- [8] S. C. Zhang and D. P. Arovas, Phys. Rev. Lett. **72**, 1886 (1994).
- [9] T. Sugiyama and N. Nagaosa, Phys. Rev. Lett. **70**, 1980 (1993).
- [10] Y. Avishai, Y. Hatsugai, and M. Kohmoto, Phys. Rev B **47**, 9561 (1993).
- [11] D. Z. Liu, X. C. Xie, S. Das Sarma, and S. C. Zhang (unpublished).
- [12] C. Pryor and A. Zee, Phys. Rev B **46**, 3116 (1992).
- [13] G. Gavazzi, J. M. Wheatley, and A. J. Schofield, Phys. Rev B **47**, 15170 (1993).
- [14] A. Barelli, R. Fleckinger, and T. Ziman, Phys. Rev B **49**, 3340 (1994).
- [15] D. K. K. Lee and J. T. Chalker, Phys. Rev. Lett. **72**, 1510 (1994).
- [16] T. Kawarabayashi and T. Ohtsuki, Phys. Rev. B (to be published).
- [17] D. N. Sheng and Z. Y. Weng (unpublished).
- [18] I speak about fractal states in a loose form, using this adjective for states in energy regions at which the mean participation ratio follows an L^α law with α smaller than the space dimension (2 in this context). Although strict fractal states certainly follow this law, self-similarity is not necessarily implied by a power law increase of the average number of sites covered by states about some fixed energy.
- [19] B. I. Shklovskii, B. Shapiro, B. R. Sears, P. Lambrianides, and H. B. Shore, Phys. Rev B **47**, 11487 (1993); V. E. Kratsov, I. V. Lerner, B. L. Altshuler, and A. G. Aronov, Phys. Rev. Lett. **72**, 888 (1994); E. Hofstetter and M. Schreiber, Phys. Rev. Lett. **73**, 3137 (1994) and, I. K. Zharekeshev and B. Kramer, Jpn. J. Appl. Phys. (to be published).
- [20] H.R. Schwarz, Numer. Math. **12**, 231 (1968).
- [21] W.H. Press, S.A. Teukolsky, W.T. Vetterling and B.P. Flannery, *Numerical Recipes* (Cambridge University Press, Cambridge, 1992).
- [22] G. Casati and L. Molinari, Phys. Rev. Lett. **64**, 1851 (1990).
- [23] C. E. Porter and R. G. Thomas, Phys. Rev **104**, 483 (1956).
- [24] V. I. Fal'ko and K. B. Efetov, (unpublished).
- [25] See, for example, *Statistical Theories of Spectra: Fluctuations*, edited by C. E. Porter, (Academic Press, New York, 1965).
- [26] Level statistics of a system belonging to the universal orthogonal class would move towards the statistics corresponding to the Gaussian Orthogonal Ensemble (GOE) whereas level statistics of a system of the universal unitary class would move towards the statistics described by the Gaussian Unitary Ensemble (GUE).
- [27] *Random Matrices*, by M. L. Mehta, (Academic Press, New York, 1991).
- [28] T. A. Brody, J. Flores, J. B. French, P. A. Mello, A. Pandey, and S. S. M. Wong, Rev. Mod. Phys. **53**, 385 (1981).
- [29] Y. V. Fyodorov and A. D. Mirlin, Phys. Rev. Lett. **67**, 2405 (1991).